

Tensor Decomposition for Non-Clifford Gate Minimization

Kirill Khoruzhii^{1,*}, Patrick Gelf¹, Sebastian Pokutta^{1,2}

¹*Zuse Institute Berlin, Berlin, Germany*

²*Technische Universität Berlin, Germany*

Fault-tolerant quantum computation requires minimizing non-Clifford gates, whose implementation via magic state distillation dominates the resource costs. While T -count minimization is well-studied, dedicated CCZ factories shift the natural target to direct Toffoli minimization. We develop algebraic methods for this problem, building on a connection between Toffoli count and tensor decomposition over \mathbb{F}_2 . On standard benchmarks, these methods match or improve all reported results for both Toffoli and T -count, with most circuits completing in under a minute on a single CPU instead of thousands of TPUs used by prior work.

DOI <https://doi.org/10.4236/ojs.202602132001> <https://github.com/khoruzhii/polytof>

1. INTRODUCTION

Fault-tolerant quantum computation relies on error correction schemes that impose vastly different costs on different gate types. In the widely adopted Clifford+ T gate set, Clifford gates can be implemented transversally in most error-correcting codes, while T gates require resource-intensive techniques such as magic state distillation [14, 27]. The resulting cost disparity is substantial: a single T gate may consume two orders of magnitude more resources than a Clifford operation [24]. This asymmetry makes non-Clifford gate minimization a central challenge in quantum circuit compilation, with direct implications for the feasibility of fault-tolerant algorithms. Beyond compilation, the T -count also governs the classical simulation complexity of quantum circuits: while Clifford circuits admit efficient simulation via the Gottesman–Knill theorem [1], adding T gates induces exponential overhead in known simulation methods [27].

Significant progress on T -count minimization has been achieved through algebraic approaches. Amy [5] established a connection between T -count optimization and coding theory, showing that the problem is equivalent to decoding Reed–Muller codes and to minimizing the symmetric tensor rank of an order-3 tensor. Building on this insight, the TODD algorithm [14] achieves substantial T -count reductions by iteratively searching for rank-reducing transformations. The recent Fast-TODD variant [27] improves computational efficiency while achieving better T -counts. These methods operate on CNOT+ T subcircuits isolated via Hadamard gadgetization [14], optimizing the Waring decomposition of the resulting signature tensor.

A different perspective emerged from AlphaTensor-Quantum [24], which applies deep reinforcement learning to tensor decomposition for circuit optimization. Beyond T -count, AlphaTensor-Quantum introduced a shifted cost model based on CCZ magic state factories [12]: when dedicated factories are available, CCZ gates (equivalently Toffoli, up to Hadamard conjugation) can be synthesized at approximately $2T$ cost rather than the naive $7T$, making direct Toffoli minimization the natural optimization target. This reframing opens a new

optimization landscape where prior T -count methods do not directly apply. However, the reinforcement learning approach requires substantial computational resources, a distributed system with over 3,600 TPU actors and training times measured in days, limiting accessibility.

Throughout this work, we follow [24] in distinguishing two cost models: the *unitary* model, where CS costs $3T$ and CCZ costs $7T$, targeting T -count minimization; and the *factory* model, where both cost $2T$, targeting Toffoli-count minimization. In the factory model, the “ T -count with gadgets” reported in [24] equals twice the Toffoli count; under this metric, our results match or improve theirs across all benchmarks.

In this work, we develop algebraic methods for Toffoli-count minimization that achieve comparable or better results with modest computational requirements; most benchmark circuits complete within a minute on a single CPU. Our approach builds on two classical problems in algebra: algebraic thickness, well-studied in cryptographic contexts [7], and canonical polyadic (CP) decomposition of order-3 tensors, central to fast matrix multiplication [10, 17]. The non-Clifford content of a circuit is captured by a cubic phase polynomial over \mathbb{F}_2 .

When CNOT and Toffoli gates are separated into distinct layers, the Toffoli count equals the algebraic thickness; optimizing only the CNOT layer before the non-Clifford part searches over $O(2^{n^2})$ basis changes. When CNOTs and Toffolis are interleaved, the minimal Toffoli count equals the CP rank; the search space grows to $O(2^{n^3})$. To find decompositions below algebraic thickness, we develop methods for direct CP rank minimization: symplectic Gaussian elimination (SGE), and flip graph search (FGS) for escaping local minima [9, 17, 19, 23]. For most benchmark circuits, separated layers suffice to match or improve prior results.

For T -count optimization, we show that CP decompositions provide effective initializations for TODD [14, 27]. Each Toffoli gate expands into seven T gates, but the resulting representation typically admits rank reduction. The diverse decompositions from the flip graph search yield starting points that outperform greedy approaches.

For bilinear circuits such as finite field multiplication, the phase polynomial has special structure that allows standard flip graph search on a smaller tensor, reducing the search space substantially. This connects to re-

* khoruzhii@zib.de

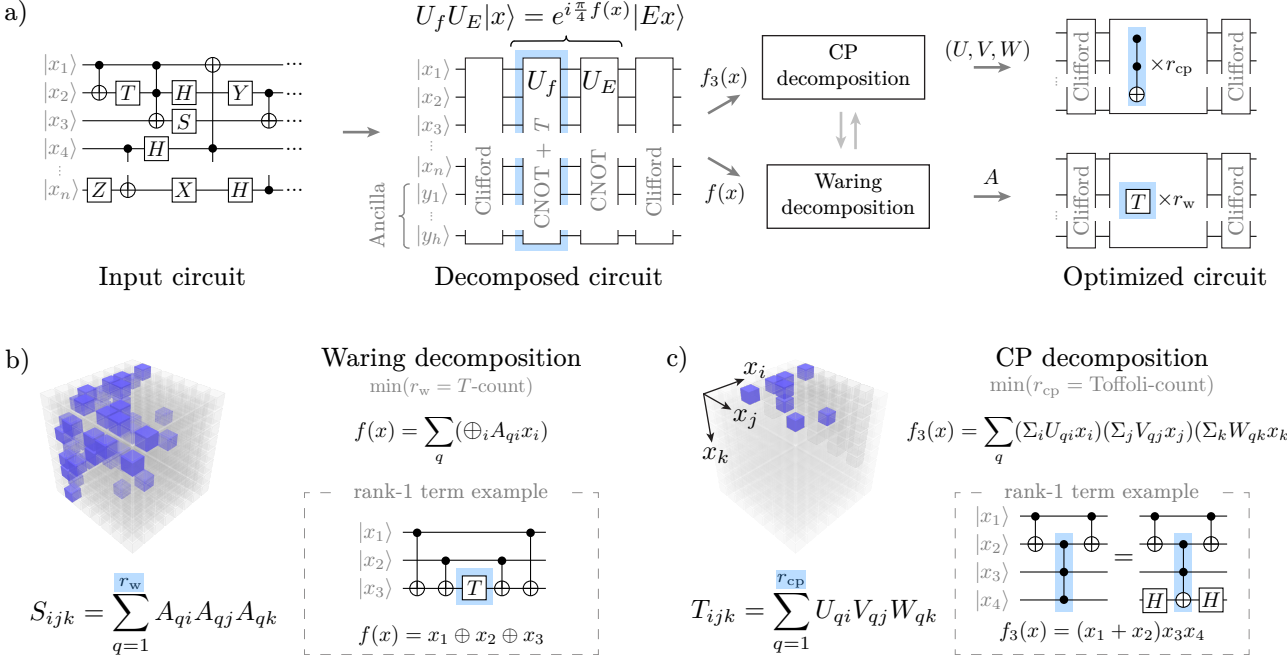


Figure 1. **Non-Clifford gate minimization as tensor decomposition.** a) Overview. Up to Clifford gates, any Clifford+ T circuit can be reduced to a diagonal phase operator U_f . Reducing non-Clifford cost is then recast as a tensor-decomposition problem: a Waring decomposition can be applied to optimize the T -count of the full phase polynomial $f(x)$, while a CP decomposition targets only the cubic part $f_3(x)$ to reduce the number of CCZ /Toffoli gates (for arithmetic circuits one often has $f = 4f_3$). In practice, a CP decomposition can serve as a useful initialization for a subsequent Waring decomposition. b) Waring decomposition. A symmetric order-3 signature tensor is written as a sum of r_w rank-1 terms, giving a realization with r_w T gates; inset shows the circuit pattern for one rank-1 term (compute a parity, apply T , uncompute). c) CP decomposition. The cubic tensor is expressed as a sum of r_{cp} rank-1 outer products, yielding an implementation with r_{cp} CCZ (equivalently Toffoli) gates acting on parity qubits. Toffoli and CCZ are interconvertible by two Hadamards as illustrated in the inset.

cent work on polynomial multiplication over \mathbb{F}_2 [9] and yields improved Toffoli counts for $GF(2^p)$ multiplication circuits.

We evaluate our methods on planted benchmarks with known structure and on standard circuit families from prior work [14, 24, 27]. Across all benchmarks, our methods match or improve prior Toffoli and T -counts with fixed hyperparameters and modest computational requirements.

This paper focuses on circuits where the phase operator can be implemented using only CNOT and CCZ gates. Since CCZ and Toffoli differ only by Hadamard conjugation, and Toffoli+ H is universal for real-valued unitaries [2, 26], this covers a broad class of quantum algorithms. Nearly all standard benchmarks fall into this setting. We do not address ancilla constraints, which merit separate investigation [27]. The underlying tensor decomposition problems are NP-hard [15], motivating the heuristic approaches developed here.

The paper is organized as follows. Sec. 2 reviews the phase polynomial representation of Clifford+ T circuits and establishes notation. Sec. 3 formalizes the connection between tensor decomposition and non-Clifford gate minimization, introducing both Waring decomposition for T -count and CP decomposition for Toffoli-count. Sec. 4 develops basis change optimization for reducing algebraic thickness. Sec. 5 presents symplectic Gaussian elimina-

tion for CP rank reduction. Sec. 6 describes flip graph search and its adaptation to cubic phase polynomials. Sec. 7 specializes to bilinear circuits, with application to finite field multiplication. Sec. 8 describes the CP initialization strategy for T -count optimization. Sec. 9 presents experimental results on planted and standard circuit benchmarks. Sec. 10 concludes with discussion of limitations and future directions. Appendices provide a proof of flip graph connectivity, a worked SGE example, details on QFT₄ optimization, and benchmark compilation specifics.

2. PHASE POLYNOMIAL REPRESENTATION

The Clifford+ T gate set provides a universal gate set for fault-tolerant quantum computation. A general Clifford+ T circuit can be systematically transformed into a canonical form that isolates the non-Clifford components. The key technique is Hadamard gadgetization [14]: each internal Hadamard gate is replaced by a gadget that consumes one ancilla qubit initialized in $|+\rangle$ and requires a Clifford correction conditioned on a measurement outcome. Since Clifford corrections commute past the non-Clifford portion (up to a change of basis), they can be deferred to the end of the circuit. After this transformation, a circuit originally acting on n qubits becomes a circuit on $n + h$ qubits, where h is the number of in-

ternal Hadamards. This process merges all non-Clifford operations into a single diagonal phase operator U_f composed of CNOT+ T gates, as shown in Fig. 1(a). Following [24, 27], we consider the regime with unlimited ancillas per circuit, focusing on minimizing non-Clifford gate count rather than qubit count.

Any CNOT+ T sequence decomposes into a phase part U_f and a linear basis transformation U_E implemented purely by CNOTs. Their action on computational basis states is

$$U_f |x\rangle = e^{i\frac{\pi}{4}f(x)} |x\rangle, \quad (1)$$

$$U_E |x\rangle = |Ex\rangle,$$

where $f : \mathbb{F}_2^n \rightarrow \mathbb{Z}_8$ is the phase function and $E \in \text{GL}(n, 2)$ is an invertible binary matrix. The non-Clifford content of the circuit is entirely captured by the phase function f , making its structure and optimization the central problem.

The phase function f arising from a CNOT+ T circuit admits a natural polynomial representation. Each T gate acts on a parity of the input qubits (determined by preceding CNOTs), contributing one term to the sum

$$f(x) = \sum_{q=1}^{r_w} \left(\bigoplus_{i=1}^n A_{qi} x_i \right), \quad (2)$$

where $A \in \mathbb{F}_2^{r_w \times n}$ is the gate synthesis matrix [14]: each row A_q encodes the parity for one T gate, and the outer sum is over integers. The number of distinct nonzero rows r_w equals the T -count; this corresponds to the Waring rank of f , discussed in Sec. 3. Conversely, any matrix A yields a CNOT+ T circuit: for each row, apply CNOTs to compute the parity on a target qubit, apply T , then reverse the CNOTs. Since the phase $e^{i\frac{\pi}{4}f(x)}$ is 2π -periodic, the function f is defined modulo 8.

To convert (2) into a standard polynomial, we use the identity

$$x_i \oplus x_j = x_i + x_j - 2x_i x_j, \quad (3)$$

which expresses XOR in terms of arithmetic operations. Applying this recursively expands any parity function into a polynomial. Since we work modulo 8, terms of degree 4 or higher vanish (they carry a factor of at least 2^3), yielding a weighted polynomial of degree at most 3:

$$f(x) = \sum_i L_i x_i + 2 \sum_{ij} Q_{ij} x_i x_j + 4 \sum_{ijk} T_{ijk} x_i x_j x_k, \quad (4)$$

which we write compactly as

$$f = f_1 + 2f_2 + 4f_3,$$

where f_1, f_2, f_3 are polynomials of degree 1, 2, and 3 with coefficients L, Q, T , respectively. The factors of 2 and 4 arise from recursive application of (3): each additional variable in a parity introduces a factor of 2 upon expansion.

The three components of the weighted polynomial correspond directly to non-Clifford gates: linear terms f_1 to T gates, quadratic terms f_2 to CS gates, and cubic terms f_3 to CCZ gates [14]. Crucially, two consecutive T gates compose to the Clifford gate S , two consecutive CS gates to CZ , and two consecutive CCZ gates cancel. Thus the non-Clifford content is precisely captured

by f_1, f_2, f_3 over \mathbb{F}_2 , and two phase operators U_f and $U_{f'}$ are Clifford-equivalent if and only if they share the same (f_1, f_2, f_3) [14].

Conversely, CS and CCZ can be expressed through T gates via (3). Matching the quadratic term gives a realization of CS using 3 T gates. For CCZ : expanding $x_i \oplus x_j \oplus x_k$ produces a term $4x_i x_j x_k$, yielding a realization using 7 T gates, which is optimal as a unitary replacement [4, 13]. Writing $|f_p|$ for the number of monomials in f_p , the total T -count for implementing f is

$$c_1|f_1| + c_2|f_2| + c_3|f_3|,$$

where the weights depend on the target cost model. For unitary decomposition into T gates, $(c_1, c_2, c_3) = (1, 3, 7)$ reflects the T -counts of T , CS , and CCZ . For magic state factory models as in [24], $(c_1, c_2, c_3) = (1, 2, 2)$ accounts for the reduced cost when dedicated factories are available [12].

For circuits with $f_1 = 0$ and $f_2 = 0$, only the CCZ count $|f_3|$ contributes to the cost, and the phase action simplifies to

$$U_f |x\rangle = (-1)^{f_3(x)} |x\rangle.$$

Such circuits appear throughout the benchmarks from [3, 14, 24, 27], particularly for arithmetic operations. The CCZ gate is related to Toffoli by conjugation with Hadamards on the target qubit:

$\text{Toffoli}_{ab \rightarrow c} = (I_a \otimes I_b \otimes H_c) \cdot CCZ_{abc} \cdot (I_a \otimes I_b \otimes H_c)$. Since Hadamards are Clifford gates, CCZ and Toffoli are interchangeable for non-Clifford gate minimization; we refer to both as Toffoli count hereafter.

In the magic state factory cost model, where Toffoli gates can be synthesized at 2 T -gate cost [12, 24], direct Toffoli-count minimization becomes the natural optimization target. This problem is closely related to multiplicative complexity (AND-count) minimization studied in the context of XAG synthesis [21, 22]. The phase polynomial formulation provides a convenient framework: Hadamard extraction reduces a $\{\text{CNOT}, \text{Toffoli}\}$ circuit to Clifford + $\{\text{CNOT}, CCZ\}$ + Clifford form, bypassing the compute/uncompute structure and ancilla management inherent in direct AND-count optimization. We develop algebraic methods for this CP decomposition problem in the following sections.

3. TENSOR DECOMPOSITION

The T -count minimization problem can be reformulated in terms of tensor decomposition. The non-Clifford content of the gate synthesis matrix A is captured by the signature tensor $S \in \mathbb{F}_2^{n \times n \times n}$, defined by

$$S_{ijk} = \sum_{q=1}^{r_w} A_{qi} A_{qj} A_{qk}. \quad (5)$$

The tensor S is symmetric and encodes the same information as (f_1, f_2, f_3) : the diagonal S_{iii} gives the linear coefficients, S_{iij} the quadratic, and S_{ijk} for distinct i, j, k the cubic [14]. Minimizing T -count is equivalent to finding a decomposition (5) with the minimum number of terms, known as the Waring decomposition [11, 24]. This construction is illustrated in Fig. 1(b).

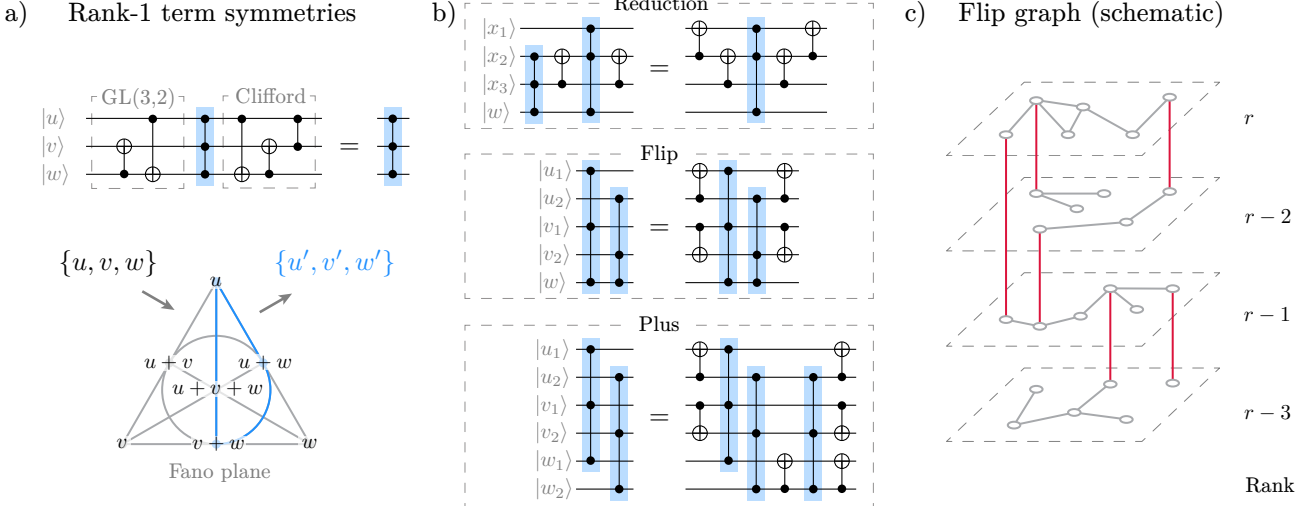


Figure 2. **Flip graph symmetries, operations, and structure.** a) Local CNOT basis changes applied before a CCZ gate can always be compensated by Clifford gates; algebraically, a cubic rank-1 term (u, v, w) depends only on the 3D subspace $\langle u, v, w \rangle$ up to $GL(3, 2)$ symmetries, visualized as a Fano plane. Any triangle (example highlighted in blue) can represent the same term. b) The flip graph is generated by three local transformations. A *reduction* decreases rank by collecting all terms over a shared factor and minimizing the induced quadratic form. A *flip* rewrites two terms sharing a common factor w while preserving rank: $u_1v_1w + u_2v_2w \mapsto (u_1+u_2)v_1w + u_2(v_1+v_2)w$. A *plus* combines an inverse reduction with a flip to escape local plateaus, temporarily increasing the rank: $u_1v_1w_1 + u_2v_2w_2 \mapsto (u_1+u_2)v_1w_1 + u_2(v_1+v_2)w_2 + u_2v_1(w_1+w_2)$. c) Schematic flip graph structure: vertices are schemes grouped by rank; horizontal edges correspond to flips within a fixed rank, vertical edges to reductions.

For CCZ -count minimization, assuming $f_1 = 0$ and $f_2 = 0$ so that $f = 4f_3$, we work with the cubic polynomial f_3 in the form

$$f_3(x) = \sum_{ijk} T_{ijk} x_i x_j x_k, \quad (6)$$

where $T \in \mathbb{F}_2^{n \times n \times n}$ is the tensor of cubic coefficients from (4). Each CCZ gate acts on three parities of the input qubits (determined by preceding CNOTs), contributing one rank-1 term (U_q, V_q, W_q) to the decomposition

$$T_{ijk} = \sum_{q=1}^{r_{cp}} U_{qi} V_{qj} W_{qk}, \quad (7)$$

where $U_q, V_q, W_q \in \mathbb{F}_2^n$ encode the three parities for one CCZ gate. This is known as a canonical polyadic (CP) decomposition [17, 20]; the CP rank r_{cp} is the CCZ count. This construction is illustrated in Fig. 1(c).

In \mathbb{F}_2 , the identity $x^2 = x$ implies that terms with linearly dependent factors reduce to quadratic and linear contributions; with the factor of 4, these are Clifford gates. This has two consequences for the CP decomposition (7). First, linearly dependent triples can be discarded; the remaining independent (U_q, V_q, W_q) can each be realized without ancillas: CNOTs compute the three parities on existing qubits, CCZ is applied, and the CNOTs are reversed. Second, each triple admits a $GL(3, 2)$ symmetry: any invertible transformation of (U_q, V_q, W_q) preserves the cubic part f_3 and adds only lower-degree (Clifford) corrections. In circuit terms, any CNOTs applied before a CCZ gate on its three qubits can be compensated by Clifford gates (Fig. 2a). The

non-Clifford content of T is thus captured by its alternating part $\text{Alt}(T)_{ijk} = S_{ijk}$, making Toffoli minimization formally a skew-symmetric tensor decomposition problem [6].

The Waring and CP decomposition problems are related: each CCZ can be realized with 7 T gates, giving $r_w \leq 7r_{cp}$. Both problems are NP-hard [10, 15, 24] in general, motivating the heuristics developed in the following sections. We begin with the simplest setting: optimizing the CNOT layer that precedes the non-Clifford gates.

4. BASIS CHANGE OPTIMIZATION

The phase polynomial can be simplified by applying a linear change of basis before the phase operator. The elementary operation

$$x_i \leftarrow x_i \oplus x_j \quad (8)$$

corresponds to a CNOT gate acting before the phase part of the circuit. Composing such elementary operations generates the full group $GL(n, 2)$ of invertible linear transformations. This corresponds to a circuit architecture where all CNOTs precede all non-Clifford gates: a basis change layer followed by a diagonal phase layer (Fig. 1). The goal is to find a basis in which the phase polynomial has fewer monomials; the minimum over all basis changes is known as the algebraic thickness [7].

Under an elementary substitution, the weighted polynomial $f = f_1 + 2f_2 + 4f_3$ transforms in a coupled manner. By the expansion (3), products involving the substituted variable acquire additional terms at higher degrees: monomials from f_1 generate contributions to f_2 , and monomials from f_2 generate contributions to f_3 . For

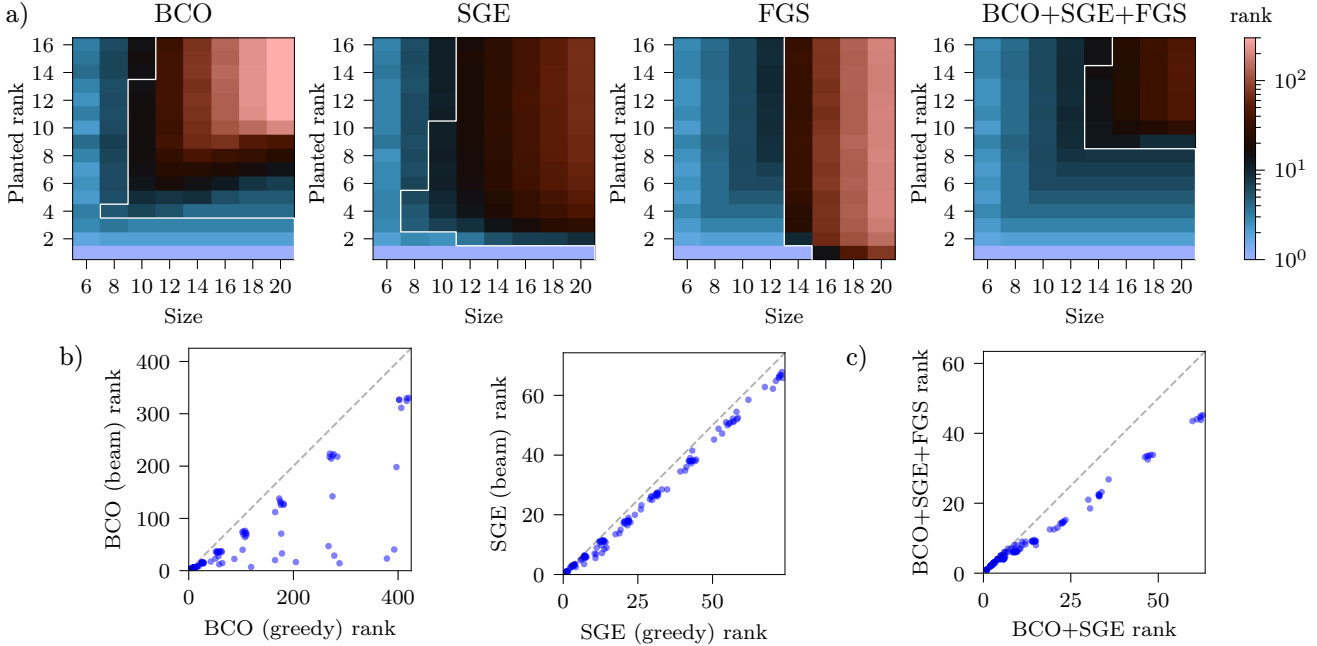


Figure 3. Performance on the planted CP benchmark. For each size and planted rank r_{pl} , we sample U, V, W uniformly and form $T_{ijk} = \sum_{q=1}^{r_{\text{pl}}} U_{qi} V_{qj} W_{qk}$. We then run the decomposition methods on T and report the recovered rank, averaged over 4 independently generated tensors for each parameter pair. a) Heatmaps show the recovered rank (logarithmic color scale) returned by BCO, SGE, FGS, and the combined pipeline BCO+SGE+FGS. The white contour separates the region where the recovered rank exceeds the planted upper bound by more than one. b) Greedy vs. beam-search variants for BCO and SGE, using beam width 2^{10} . c) Rank improvement from FGS after BCO+SGE. Dashed lines indicate equality.

circuits with $f_1 = 0$ and $f_2 = 0$, the optimization reduces to minimizing the number of cubic monomials $|f_3|$. In this case, each monomial $x_i x_j x_k$ requires one CCZ gate, so the Toffoli count equals $|f_3|$. Algebraic thickness thus provides an upper bound on the CP rank: separated layers are a special case of interleaved circuits, and allowing CNOTs between CCZ gates can achieve lower counts.

Exhaustive search over $\text{GL}(n, 2)$ is infeasible: the group has order $|\text{GL}(n, 2)| = \prod_{k=0}^{n-1} (2^n - 2^k)$, which exceeds 10^{12} already for $n = 8$. We therefore employ heuristic search strategies.

In the greedy approach, we iteratively select the elementary substitution that maximally decreases the cost function, terminating when no improvement is possible. Each step considers $n(n - 1)$ candidates, making individual iterations efficient. To escape local minima, we also consider beam search: at each step, we maintain a pool of the top k candidates (ranked by cost) and expand each by all possible single substitutions, retaining the best k results for the next iteration. Fig. 3b compares the performance of greedy and beam search variants on synthetic benchmarks.

However, algebraic thickness and CP rank are not equal in general. A minimal example is

$$f_3 = x_1 x_3 x_5 + x_1 x_3 x_6 + x_1 x_4 x_6 + x_2 x_3 x_6 + x_2 x_4 x_5,$$

which has algebraic thickness 5 (no basis change reduces the monomial count [16]) but $r_{\text{cp}} = 3$ with decomposition

$$f_3 = x_1 x_3 x_5 + (x_1 + x_2)(x_3 + x_4)x_6 + x_2 x_4(x_5 + x_6).$$

Despite this gap, basis change optimization (BCO) proves

effective as a preprocessing step before direct CP decomposition methods such as SGE (Sec. 5) and FGS (Sec. 6). For most benchmarks from prior work [24], BCO alone is sufficient to match or improve upon prior results.

5. QUADRATIC FORM REDUCTION

The $\text{GL}(3, 2)$ symmetry of rank-1 terms allows reducing the CCZ count by grouping terms that share a common factor. When multiple terms contain the same element in their subspace, the combined contribution factorizes into a product of a linear form and a quadratic form; minimizing CCZ count then reduces to minimizing the rank of this quadratic form.

Each rank-1 term (u, v, w) in a CP decomposition spans a 3-dimensional subspace $\langle u, v, w \rangle$. The seven nonzero elements of this subspace form the *seven-set*:

$$\mathcal{S} = \{u, v, w, u + v, u + w, v + w, u + v + w\}. \quad (9)$$

Any triple of linearly independent vectors from \mathcal{S} generates the same subspace and thus represents the same term up to Clifford equivalence. Geometrically, these seven elements correspond to the seven points of the Fano plane, and the 28 valid triples correspond to its triangles (Fig. 2a).

For a fixed vector z , let $\mathcal{T}_z = \{q : z \in \mathcal{S}_q\}$ be the set of all terms whose seven-set contains z . For each such term, the $\text{GL}(3, 2)$ symmetry allows choosing a representative triple (u_q, v_q, z) with z as the common factor. The combined contribution to f_3 then factorizes as $(z \cdot x)$ times a

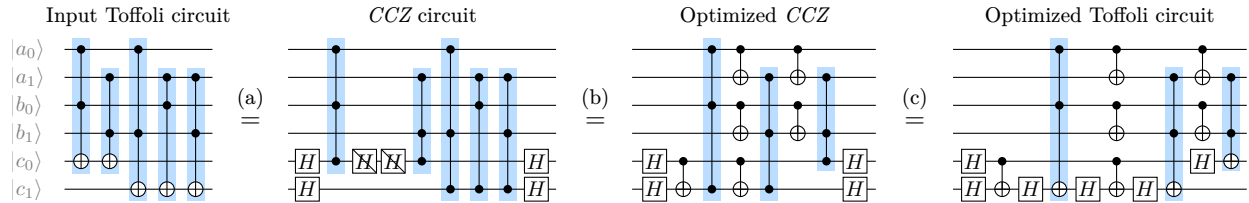


Figure 4. **Bilinear circuit optimization pipeline.** The example shows a $GF(2^2)$ multiplication circuit. (a) Hadamard conjugation on the output register converts Toffoli gates to CCZ gates; adjacent H gates cancel. (b) Low-rank CP decomposition of the bilinear tensor reduces the CCZ count from 5 to 3. (c) Inverse Hadamard conjugation restores Toffoli form.

quadratic form in x :

$$\sum_{q \in \mathcal{T}_z} (u_q \cdot x)(v_q \cdot x) = \sum_{i < j} B_{ij} x_i x_j,$$

where B is the alternating matrix:

$$B_{ij} = \sum_{q \in \mathcal{T}_z} (u_{qi} v_{qj} + u_{qj} v_{qi}). \quad (10)$$

Any alternating matrix can be brought to a canonical block-diagonal form via congruence $B \mapsto S^T B S$ using symplectic Gaussian elimination (SGE) in $O(n^3)$ time [29]. SGE performs row and column additions simultaneously (adding row j to row i together with column j to column i), preserving symmetry while reducing to canonical form. The result consists of r blocks $\begin{pmatrix} 0 & 1 \\ 1 & 0 \end{pmatrix}$ followed by zeros; each block corresponds to one CCZ gate, so the $|\mathcal{T}_z|$ original terms sharing factor z reduce to r terms. A worked example appears in Appendix 11B.

The reduction procedure is applied iteratively, selecting at each step a vector z appearing in at least two seven-sets. In greedy mode, we choose the z that maximizes $|\mathcal{T}_z| - r$. In beam search mode, as in BCO (Sec. 4), we maintain a pool of the top k decompositions, expanding each by all improving reductions and retaining the best k results. The search terminates when no choice of z reduces the rank.

For all benchmark cubic circuits in Table 1, BCO followed by SGE suffices to match or improve upon prior results. When SGE reaches a local minimum, flip graph search (Sec. 6) provides a mechanism to escape it.

6. FLIP GRAPH SEARCH

Flip graph search explores rank-preserving transformations to escape local minima where no shared factor admits further reduction. This approach adapts the framework developed for matrix multiplication [17, 23] to the CP decomposition of cubic phase polynomials.

The flip graph at rank r has vertices corresponding to CP decompositions of the target cubic polynomial with exactly r terms. Edges are generated by three local transformations (Fig. 2b). A *flip* is a rank-preserving transformation that rewrites two terms sharing a common factor: given (u_1, v_1, z) and (u_2, v_2, z) , the flip replaces them with $(u_1 + u_2, v_1, z)$ and $(u_2, v_1 + v_2, z)$. Both configurations contribute the same cubic polynomial when expanded, but the new decomposition may have different shared factors, potentially enabling reductions that were

previously unavailable. A *reduction* decreases the rank by applying SGE to all terms sharing a common factor z , as described in Sec. 5. A *plus* transition [17] temporarily increases the rank to escape local plateaus; it applies to two terms with disjoint seven-sets, introducing a third term that creates new shared factors and subsequent flip opportunities (Fig. 2b).

The search proceeds via random walks on the flip graph, following the framework of [17, 19, 23]. We maintain a pool of $S = 10^3$ decompositions at the current rank r . Each iteration selects a random decomposition from the pool and performs a random walk seeking rank $r-1$ or lower. At each step, we sample a random flip from available candidates. If the walk stagnates for $P = 5 \times 10^4$ consecutive steps without finding a reduction, we attempt a plus transition to escape the local plateau. The walk terminates after at most $L = 10^6$ steps or upon reaching a lower rank. When a walk successfully reaches rank $r-1$, the resulting decomposition is added to the next-level pool; once this pool accumulates S decompositions, we advance to rank $r-1$ and repeat. The search terminates when no walks succeed in reducing the rank further.

Reductions are detected at two granularities. During flips, if two terms have seven-sets intersecting in 3 or 7 elements, the rank decreases by 1 or 2 respectively; such reductions are applied immediately with negligible computational overhead. Full SGE iterations, which scan all shared factors, are more expensive and performed every $R = 10^4$ steps.

Maintaining a diverse pool is essential: different decompositions at the same rank may occupy different regions of the flip graph, and reductions can lead to isolated components with no further descent paths (Fig. 2c). The plus transition provides an additional mechanism to bridge such components by temporarily increasing rank before finding alternative descent paths (Appendix 11 A). All experiments use the parameters above; preliminary experiments suggest the method is robust to their variation, though larger pool sizes and walk lengths may enable reaching lower ranks at increased computational cost. Our implementation achieves approximately 10^6 flip steps per second per thread.

7. BILINEAR APPROACH

For circuits implementing bilinear maps, such as finite field multiplication, flip graph search can operate directly on smaller tensors with improved efficiency. This bilin-

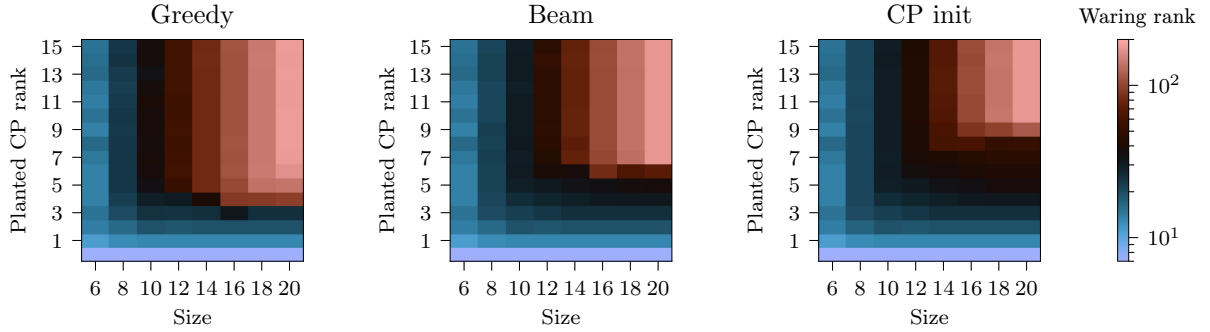


Figure 5. Waring decomposition performance on planted CP benchmark. For the same planted CP tensors T from Fig. 3, we then seek a minimal Waring decomposition of the signature tensor $S = \text{Alt}(T)$. We compare three approaches: greedy selection from the original FastTODD [27], beam search with width 2^{10} , and greedy selection with CP initialization. Results show the recovered Waring rank r_w averaged over 4 independently generated tensors.

ear complexity setting, familiar from matrix multiplication [17] and polynomial multiplication [9], admits direct application to quantum circuits.

A quantum circuit implementing a bilinear map performs the transformation

$$|a, b, c\rangle \mapsto |a, b, c \oplus g(a, b)\rangle,$$

where each output bit c_k is a bilinear function of the inputs:

$$c_k \mapsto c_k \oplus \sum_{ij} G_{ijk} a_i b_j.$$

Each term $c_k \oplus a_i b_j$ corresponds to one Toffoli gate with target on c_k .

After expressing each Toffoli gate as Hadamard-conjugated CCZ (Sec. 2), adjacent Hadamards cancel pairwise, leaving H gates only at the circuit boundaries (Fig. 4). The remaining non-Clifford part implements a pure phase polynomial

$$f_3 = \sum_{ijk} G_{ijk} a_i b_j c_k.$$

A CP decomposition $G_{ijk} = \sum_{q=1}^r U_{qi} V_{qj} W_{qk}$ then corresponds directly to a circuit with r CCZ gates: minimizing the Toffoli count is equivalent to minimizing the CP rank of G .

Unlike the cubic phase polynomial setting, the tensor G has dimensions (n_a, n_b, n_c) rather than (n, n, n) for $n = n_a + n_b + n_c$, and the $\text{GL}(3, 2)$ symmetry does not apply. This is the standard bilinear setting of the original flip graph framework [17]. Flips operate on pairs of terms sharing a common factor along any of the three axes, and plus transitions introduce a third term from two terms with no shared factors. Reductions occur when terms with a shared factor have linearly dependent vectors along another axis, allowing terms to be combined. The search procedure and parameters follow Sec. 6.

We now specialize to finite field multiplication circuits, the primary application of this approach. Elements of $\text{GF}(2^p)$ are represented as polynomials $a(x) = \sum_{k=0}^{p-1} a_k x^k$ with binary coefficients, and multiplication is performed modulo an irreducible polynomial $h(x)$ of

degree p . The quantum circuit implements

$$|a, b, c\rangle \mapsto |a, b, c \oplus (a(x) \cdot b(x) \bmod h(x))\rangle,$$

which decomposes into two stages with distinct tensor representations.

Polynomial multiplication computes $a(x)b(x)$ of degree at most $2p - 2$ via the convolution $(ab)_\ell = \sum_{i+j=\ell} a_i b_j$, defining the *convolution tensor* $G^{\text{conv}} \in \mathbb{F}_2^{p \times p \times (2p-1)}$ with $G_{ij\ell}^{\text{conv}} = 1$ iff $i + j = \ell$. Modular reduction $ab \bmod h$ is a linear map $R : \mathbb{F}_2^{2p-1} \rightarrow \mathbb{F}_2^p$ requiring no additional a - b multiplications. Composing both stages yields the *field tensor* $G^{\text{GF}} \in \mathbb{F}_2^{p \times p \times p}$ for $\text{GF}(2^p)$ multiplication:

$$G_{ijk}^{\text{GF}} = \sum_{\ell} G_{ij\ell}^{\text{conv}} R_{k\ell}.$$

Any rank- r decomposition of G^{conv} with factors (U_q, V_q, W_q) induces a rank- r decomposition of G^{GF} by projecting $W'_{qj} = R_{kl} W_{lq}$. A decomposition of G^{GF} embeds directly into a phase polynomial circuit: the transformation $(i, j, k) \mapsto (i, p+j, 2p+k)$ maps the $p \times p \times p$ field tensor to a $3p \times 3p \times 3p$ tensor representing f_3 , with factors supported on disjoint index blocks $[0, p)$, $[p, 2p)$, $[2p, 3p)$ corresponding to a , b , c registers.

We can therefore optimize either tensor: decompositions of G^{conv} project to valid G^{GF} decompositions, while searching G^{GF} directly explores a more constrained space where the modular structure may enable lower ranks. For polynomial multiplication alone, Karatsuba-style recursive decompositions achieve $O(p^{\log_2 3})$ rank, as observed in quantum circuit constructions [24, 28]. Flip graph search over \mathbb{F}_2 was recently applied to G^{conv} [9], finding decompositions that improve upon [24, 28]. Our bilinear approach matches or improves upon all prior automated results [24] and reproduces most bounds of [9]; searching the field tensor G^{GF} directly can yield lower ranks than the convolution tensor alone, e.g. rank 15 versus 17 for $p = 6$. We run both formulations and report the best in Table 2.

8. T-COUNT OPTIMIZATION

For circuits with $f = 4f_3$, Toffoli-count minimization via CP decomposition is the natural optimization tar-

Table 1. **Benchmark results for non-Clifford gate minimization.** Comparison of Toffoli-count (via CP decomposition) and T -count (via Waring decomposition) optimization on circuits from [24]. For Toffoli minimization, flip graph search (this work) generates 10^3 candidate schemes in time t ; for T minimization, each scheme initializes a run of our implementation of TODD [14] with the modifications from [27]. Bold entries indicate improvements over best prior results. Grey entries in Toffoli-count indicate use of additional non-Clifford gates (T, CS) beyond Toffoli. † Result obtained using BCO+SGE; unmarked entries use BCO only.

| Circuit | n | h | Size | Toffoli-minimization (r_{cp}) | | | | | | T-minimization (r_w) | | | |
|---------------------------|-----|-----|------|-----------------------------------|-------|-------|-----------|-------|-------------------------|-------------------------------|-----------------------|------------|--|
| | | | | Best prior ^[24] | | | This work | | | Best prior ^[24,27] | | This work | |
| | | | | $+T$ | $+CS$ | Count | $+T$ | $+CS$ | Count | t, s | Count | Count | |
| Adders ₈ | 24 | 37 | 61 | 28 | | 33 | | | 27 [†] | 68 | 119 ^[27] | 117 | |
| Barenco Tof ₃ | 5 | 3 | 8 | | | 2 | | | 2 | 0 | 13 ^[24,27] | 13 | |
| Barenco Tof ₄ | 7 | 7 | 14 | | | 4 | | | 4 | 1 | 23 ^[24,27] | 23 | |
| Barenco Tof ₅ | 9 | 11 | 20 | | | 6 | | | 6 | 1 | 33 ^[24,27] | 33 | |
| Barenco Tof ₁₀ | 19 | 31 | 50 | | | 16 | | | 16 | 12 | 83 ^[24,27] | 83 | |
| CSLA MUX ₃ | 15 | 6 | 21 | | | 8 | | | 8 | 1 | 39 ^[24,27] | 39 | |
| CSUM MUX ₉ | 30 | 12 | 42 | | | 14 | | | 14 | 6 | 71 ^[24,27] | 71 | |
| Grover ₅ | 9 | 68 | 77 | 12 | | 27 | | | 25 | 101 | 143 ^[27] | 143 | |
| Ham ₁₅ (low) | 17 | 25 | 42 | | | 17 | | | 17 | 16 | 73 ^[24] | 73 | |
| Ham ₁₅ (med) | 17 | 54 | 71 | 8 | | 35 | | | 33 [†] | 24 | 137 ^[27] | 137 | |
| Ham ₁₅ (high) | 20 | 331 | 351 | 90 | 2 | 173 | | | 156 [†] | 3430 | 643 ^[27] | 643 | |
| HWB ₆ | 7 | 20 | 27 | | | 10 | | | 10 [†] | 3 | 51 ^[24,27] | 51 | |
| Mod 5 ₄ | 5 | 0 | 5 | | | 1 | | | 1 | 0 | 7 ^[24,27] | 7 | |
| Mod Adder ₁₀₂₄ | 28 | 304 | 331 | 188 | 15 | 141 | | | 128 | 15800 | 575 ^[27] | 573 | |
| Mod Mult ₅ | 9 | 2 | 11 | | | 3 | | | 3 | 0 | 17 ^[24,27] | 17 | |
| Mod Red ₂₁ | 11 | 17 | 28 | | | 11 | | | 11 | 4 | 51 ^[24,27] | 51 | |
| QCLA Adder ₁₀ | 36 | 25 | 61 | 28 | 5 | 28 | | | 24 | 5 | 109 ^[27] | 107 | |
| QCLA Com ₇ | 24 | 18 | 42 | | | 12 | | | 12 | 11 | 59 ^[24,27] | 59 | |
| QCLA Mod ₇ | 26 | 58 | 84 | 36 | | 43 | | | 37 | 55 | 159 ^[27] | 153 | |
| QFT ₄ | 5 | 38 | 43 | 30 | 3 | 4 | 29 | 3 | 4 | 10 | 53 ^[24,27] | 53 | |
| RC Adder ₆ | 14 | 10 | 24 | | | 6 | | | 6 | 2 | 37 ^[24,27] | 37 | |
| Tof ₃ | 5 | 2 | 7 | | | 2 | | | 2 | 0 | 13 ^[24,27] | 13 | |
| Tof ₄ | 7 | 4 | 11 | | | 3 | | | 3 | 1 | 19 ^[24,27] | 19 | |
| Tof ₅ | 9 | 6 | 15 | | | 4 | | | 4 | 1 | 25 ^[24,27] | 25 | |
| Tof ₁₀ | 19 | 16 | 35 | | | 9 | | | 9 | 7 | 55 ^[24,27] | 55 | |
| VBE Adder ₃ | 10 | 4 | 14 | | | 3 | | | 3 | 1 | 19 ^[24,27] | 19 | |

Table 2. **Benchmark results for $GF(2^p)$ multiplication circuits.** For prior work, Auto denotes automatic optimization; Overall reports best known results, including hand-crafted Karatsuba-style constructions and multiplicative complexity bounds from [8, 9], transferred to quantum circuits as in Fig. 4. For Toffoli minimization, General applies SGE+FGS to the phase tensor without exploiting circuit structure, while Bilinear leverages the bilinear map structure to work directly with smaller tensors G^{GF} or G^{conv} . For T minimization, we use our implementation of TODD [14] with the modification from [27], initialized from CP decompositions: Auto uses decompositions obtained by General and Bilinear approaches, while +MC uses known multiplicative complexity constructions from [8]. Bold entries improve upon best prior results. *Result not achieved in every run (at least 1 of 10). † Requires Bilinear initialization. ‡ Requires BCO preprocessing and General approach.

| Circuit | Size | Toffoli minimization (r_{cp}) | | | | | | T minimization (r_w) | | | | |
|-------------------|------|-----------------------------------|-------------------|---------|-----------|----------------------|----------------------|----------------------------|------------------|--------------------|-----------|--|
| | | Best prior | | | This work | | | Best prior | | | This work | |
| | | Auto ^[24] | Overall | General | Bilinear | Auto ^[24] | Auto ^[27] | Overall ^[24,27] | Auto | +MC ^[8] | | |
| $GF(2^2)$ Mult | 6 | 3 | $3^{[8,9,24,27]}$ | 3 | 3 | 17 | 18 | $17^{[24,27]}$ | 17 | 17 | | |
| $GF(2^3)$ Mult | 9 | 6 | $6^{[8,9,24,27]}$ | 6 | 6 | 29 | 36 | $23^{[27]}$ | 29 | 29 | | |
| $GF(2^4)$ Mult | 12 | 9 | $9^{[8,9,24,27]}$ | 9 | 9 | 39 | 49 | $39^{[24]}$ | 39* | 45 | | |
| $GF(2^5)$ Mult | 15 | 13 | $13^{[8,9,24]}$ | 13 | 13 | 59 | 81 | $59^{[24]}$ | $59^{*\ddagger}$ | 63 | | |
| $GF(2^6)$ Mult | 18 | 18 | $15^{[8]}$ | 15^* | 15 | 77 | 113 | $77^{[24]}$ | 77^\dagger | 81 | | |
| $GF(2^7)$ Mult | 21 | 22 | $22^{[8,9,24]}$ | 23^* | 22 | 104 | 155 | $104^{[24]}$ | 101^\dagger | 103 | | |
| $GF(2^8)$ Mult | 24 | 29 | $24^{[8]}$ | 34^* | 26 | 123 | 205 | $123^{[24]}$ | $123^{\dagger*}$ | 127 | | |
| $GF(2^9)$ Mult | 27 | 35 | $30^{[8]}$ | 51^* | 32^* | 161 | 257 | $161^{[24]}$ | $153^{\dagger*}$ | 147 | | |
| $GF(2^{10})$ Mult | 30 | 46 | $33^{[8]}$ | 66^* | 39 | 196 | 315 | $196^{[24]}$ | 185^\dagger | 173 | | |

get when *CCZ* magic state factories are available, as each *CCZ* costs only $2T$ [24]. Without such factories, the standard cost model assigns $7T$ per *CCZ*, making further T -count reduction worthwhile. This section describes how CP decompositions serve as initialization for Waring decomposition algorithms, and presents modifications to TODD [14, 27] that improve T -count results.

Each CP term (u, v, w) contributing to f_3 expands into seven Waring terms:

$$\{u, v, w, u \oplus v, u \oplus w, v \oplus w, u \oplus v \oplus w\}. \quad (11)$$

This gives the naive bound $r_w \leq 7r_{\text{cp}}$ from Sec. 3, but the expanded representation typically admits further rank reduction.

TODD [14, 27] is currently the best-performing heuristic for T -count minimization via Waring decomposition. The goal is to reduce the number of rows in the gate synthesis matrix A while preserving the signature tensor (5).

At each iteration, TODD searches for a rank-reducing transformation of the form

$$A \leftarrow A \oplus yz^T,$$

where $y \in \mathbb{F}_2^{r_w}$ selects rows and $z \in \mathbb{F}_2^n$ is XORed into them. If two rows become equal or a row becomes zero, they can be removed. The algorithm proceeds greedily: at each step, it selects the (y, z) pair that maximizes rank reduction, applies the transformation, and recurses until no further reduction is possible.

Greedy algorithms are sensitive to initialization. The flip graph search (Sec. 6) typically produces around 10^3 distinct CP decompositions in our setting; expanding each via (11) yields diverse starting points for TODD. Different decompositions lead the algorithm into different regions of the search space, while the CP-derived initializations themselves typically have lower rank than naive expansion.

Fig. 5 evaluates initialization strategies on planted Waring instances. On these planted instances, CP initialization consistently outperforms both naive greedy and beam search, often by a substantial margin; on real benchmark circuits (Table 1), the improvements are more modest but still present. Notably, adding beam search to CP initialization yields no further improvement: diverse starting points from the flip graph appear to compensate for the lack of within-run exploration.

9. RESULTS

We evaluate the proposed methods on planted benchmarks with known structure and on standard benchmark circuits from prior work [24, 28]. Planted instances provide controlled settings where the target rank is known, enabling direct assessment of recovery quality. Benchmark circuits allow comparison with prior optimization results. All experiments use fixed FGS hyperparameters (pool size $S = 10^3$, walk length $L = 10^6$, SGE iteration interval $R = 10^4$) across all instances. Beam search variants use width 2^{10} throughout. Computations were performed on a 48-core Intel Xeon Gold 6246 processor with a 24-hour time limit.

To validate the optimization pipeline, we construct in-

stances with known CP structure. For each pair of dimension n and planted rank r_{pl} , we sample factor matrices $U, V, W \in \mathbb{F}_2^{r_{\text{pl}} \times n}$ uniformly at random and form the tensor (7). The planted rank r_{pl} provides an upper bound on the true CP rank, which may be lower due to cancellations. We apply the decomposition methods and report the recovered rank, averaged over 4 independently generated tensors for each parameter pair. Fig. 3a presents heatmaps of recovered rank across the (n, r_{pl}) parameter space for each method and their combination. BCO and SGE use beam search. BCO alone recovers low ranks for small tensors but reaches a plateau as dimension and rank increase. Adding SGE extends the region of successful recovery, and adding FGS further expands this region. Fig. 3b compares greedy and beam search variants for BCO and SGE, showing consistent improvement from maintaining multiple candidates. Fig. 3c isolates the contribution of FGS by plotting recovered rank after BCO+SGE+FGS against BCO+SGE alone. The planted benchmarks reveal that problem difficulty depends not only on circuit size but also on the underlying tensor rank.

The same planted instances provide a testbed for T -count optimization via Waring decomposition. Given a planted tensor T with CP rank r_{pl} , the signature tensor $S = \text{Alt}(T)$ admits Waring decompositions with rank at most $7r_{\text{pl}}$. We compare three strategies for TODD: greedy selection with naive initialization, beam search, and greedy selection with CP initialization from BCO+SGE+FGS. Fig. 5 presents the recovered Waring rank r_w . CP initialization consistently outperforms both greedy and beam search, often by a substantial margin. Notably, beam search with CP initialization yields no significant improvement over the greedy approach.

Table 1 presents results on 25 benchmark circuits from [24]. For Toffoli minimization, BCO+SGE with beam search improves upon the best prior results in 8 of 25 circuits, with the remaining circuits matching prior performance. For T -count minimization, TODD benefits from diverse initializations, thus we use SGE (greedy) + FGS, which produces up to 10^3 distinct CP decompositions, all used to initialize TODD. This yields T -count improvements in 5 circuits.

The computational requirements contrast sharply with reinforcement learning approaches. AlphaTensor-Quantum requires a distributed system with over 3,600 TPU actors, with training times measured in days [24]. Our method requires no training and runs on a single CPU; most circuits complete in seconds to minutes, with the largest requiring several hours.

For pure cubic phase polynomials, AlphaTensor-Quantum sometimes requires circuit splitting due to scalability constraints, producing mixed gate sets with T and CS gates alongside Toffoli. Our approach optimizes the full phase polynomial directly without splitting, following [27], yielding pure Toffoli implementations with equal or lower Toffoli counts.

Table 2 presents results for $\text{GF}(2^p)$ multiplication circuits. These circuits implement bilinear maps and proved challenging for AlphaTensor-Quantum as well, requiring a modified training procedure [24]. We consider two op-

timization approaches: general phase polynomial methods (BCO+SGE+FGS applied to the full $(3p, 3p, 3p)$ tensor) and the bilinear formulation working directly with the smaller field tensor (p, p, p) or convolution tensor $(p, p, 2p-1)$. The general approach matches prior results for small fields ($p \leq 6$) but struggles for larger instances. The bilinear formulation substantially reduces the search space and succeeds where the general approach does not. For $p \geq 6$, we performed 10 independent runs per circuit; entries marked with * indicate the minimum observed rank, not achieved in every run. For $\text{GF}(2^p)$ multiplication, multiplicative complexity (AND-count) equals Toffoli count since control and target registers occupy disjoint qubits; dedicated algebraic constructions from [8] can therefore be transferred to quantum circuits as in Fig. 4. For $p = 8, 9, 10$ these bounds remain below our automatic results. Using these constructions as CP initialization for TODD with beam width 2^{10} yields improved T -counts for $p = 9, 10$.

The original work [24] includes an additional benchmark suite of 35 circuits spanning binary addition, Hamming weight computation, phase gradients, unary iteration, and quantum chemistry primitives, with sizes up to 72 qubits. On all 35 circuits, BCO+SGE recovers pure Toffoli implementations matching the reported Toffoli counts within one minute, without requiring FGS.

Together, these experiments cover all benchmarks from [24], matching or improving prior results across all circuit families.

10. DISCUSSION

We have demonstrated that algebraic methods for quantum circuit optimization achieve results matching or exceeding state-of-the-art reinforcement learning while requiring orders of magnitude less computation. We attribute this efficiency to restricting the search space to modifications of correct circuit implementations while retaining flexibility to reach low-rank decompositions.

For structured circuit families such as finite field multiplication, specialized formulations that exploit known structure substantially outperform general methods. The bilinear approach reduces the search space from tensors of dimension $(3p, 3p, 3p)$ to (p, p, p) , an exponential reduction. This principle likely extends to other circuit classes, for example through quadratization of higher-degree polynomials.

For finite field multiplication, known multiplicative complexity constructions [8] provide Toffoli counts below our automatic results for larger fields. These constructions are typically recursive, building decompositions for $\text{GF}(2^p)$ from smaller building blocks. In the context of matrix multiplication, the meta flip graph [18] systematically exploits this recursive structure, composing small decompositions into larger ones. We expect that adapting this framework to finite field arithmetic may yield improvements beyond existing constructions by combining structured recursion with automatic search.

Interestingly, AlphaTensor-Quantum also found $\text{GF}(2^p)$ circuits particularly challenging among their

benchmarks. Their solution was to modify the training procedure to force Toffoli gadgets, effectively steering the search toward CP-like decompositions rather than general Waring decompositions [24]. This aligns with our observation that specialized structure, when available, should be exploited directly. More broadly, it suggests that CP decomposition may be a more natural optimization target than Waring decomposition for circuit classes with bilinear structure, echoing the original AlphaTensor approach to matrix multiplication [10].

More broadly, Toffoli-count minimization via phase polynomials is closely related to multiplicative complexity minimization in classical circuit synthesis. Prior work connecting multiplicative complexity to T -count [21, 22] reported higher AND-counts than our Toffoli counts on overlapping benchmarks, and consequently higher T -counts. This is consistent with the findings of [27], where omitting ancilla introduction for Hadamard extraction, and thus not merging non-Clifford gates into a single phase operator, led to consistently higher T -counts. The phase polynomial framework also offers advantages by working with CCZ gates directly and eliminating compute/uncompute considerations, though extending our methods to work in the XAG setting remains a natural direction.

Several methodological extensions merit investigation. Extending flip graph concepts to Waring decomposition, through walks that traverse decompositions of equal rank with occasional rank increases, could improve T -count optimization directly rather than relying on CP initialization. The interplay between local operations such as flips and global transformations as in TODD deserves further study for both CP and Waring decomposition. More immediately, scaling to larger circuits following [28] and incorporating ancilla constraints that induce different phase polynomial partitions are natural next steps. Optimizing non-Clifford depth [25] rather than count alone is another practical direction, as circuit depth directly impacts execution time in fault-tolerant architectures. Handling mixed-degree phase polynomials, where linear and quadratic terms interact with cubic terms, remains underdeveloped beyond the approach used for QFT_4 (Appendix 11 C).

We deliberately kept hyperparameters fixed across all experiments to demonstrate out-of-the-box performance: a method accessible on a laptop without per-instance tuning. All circuits and decompositions reported in Table 1, Table 2 and additional benchmarks are released together with the full search code and runnable examples in a public repository `polytof`. The C++ implementation is self-contained with no external dependencies and includes utilities to reproduce all results, verification scripts, and examples for optimizing new circuits.

Finally, we suggest that structured algebraic approaches define search spaces where learned heuristics can operate more effectively. The flip graph and the space of basis changes are natural candidates for integration with neural network guidance and reinforcement learning, potentially yielding further improvements with far less computational overhead than learning from scratch.

ACKNOWLEDGMENTS

This research was supported by the DFG Cluster of Excellence MATH+ (EXC-2046/1, project id 390685689) funded by the Deutsche Forschungsgemeinschaft (DFG), as well as by the National High-Performance Computing (NHR) network.

REFERENCES

[1] S. Aaronson and D. Gottesman. Improved Simulation of Stabilizer Circuits. *Physical Review A*, 70(5):052328, Nov. 2004.

[2] D. Aharonov. A Simple Proof that Toffoli and Hadamard are Quantum Universal, Jan. 2003.

[3] M. Amy and J. Lundervile. Linear and Non-linear Relational Analyses for Quantum Program Optimization. *Proceedings of the ACM on Programming Languages*, 9(POPL):1072–1103, Jan. 2025.

[4] M. Amy, D. Maslov, M. Mosca, and M. Roetteler. A Meet-in-the-Middle Algorithm for Fast Synthesis of Depth-Optimal Quantum Circuits. *IEEE Transactions on Computer-Aided Design of Integrated Circuits and Systems*, 32(6):818–830, June 2013.

[5] M. Amy and M. Mosca. T-count optimization and Reed-Muller codes. *IEEE Transactions on Information Theory*, 65(8):4771–4784, Aug. 2019.

[6] E. Arrondo, A. Bernardi, P. M. Marques, and B. Mourrain. Skew-Symmetric Tensor Decomposition. *Communications in Contemporary Mathematics*, 23(02):1950061, Mar. 2021.

[7] C. Carlet. On Cryptographic Complexity of Boolean Functions. In G. L. Mullen, H. Stichtenoth, and H. Tapia-Recillas, editors, *Finite Fields with Applications to Coding Theory, Cryptography and Related Areas*, pages 53–69, Berlin, Heidelberg, 2002. Springer.

[8] M. Cenk and F. Özbudak. On multiplication in finite fields. *Journal of Complexity*, 26(2):172–186, Apr. 2010.

[9] S. Chen and M. Kauers. Flip Graphs for Polynomial Multiplication, Feb. 2025.

[10] A. Fawzi, M. Balog, A. Huang, T. Hubert, B. Romera-Paredes, M. Barekatain, A. Novikov, F. J. R. Ruiz, J. Schrittweiser, G. Swirszcz, D. Silver, D. Hassabis, and P. Kohli. Discovering faster matrix multiplication algorithms with reinforcement learning. *Nature*, 610(7930):47–53, Oct. 2022.

[11] R. Fröberg, G. Ottaviani, and B. Shapiro. On the Waring problem for polynomial rings. *Proceedings of the National Academy of Sciences*, 109(15):5600–5602, Apr. 2012.

[12] C. Gidney and A. G. Fowler. Efficient magic state factories with a catalyzed $|ccz\rangle$ to $2|t\rangle$ transformation. *Quantum*, 3:135, Apr. 2019.

[13] D. Gosset, V. Kliuchnikov, M. Mosca, and V. Russo. An algorithm for the T-count. *Quantum Info. Comput.*, 14(15-16):1261–1276, Nov. 2014.

[14] L. E. Heyfron and E. T. Campbell. An efficient quantum compiler that reduces T count. *Quantum Science and Technology*, 4(1):015004, Sept. 2018.

[15] C. J. Hillar and L.-H. Lim. Most Tensor Problems Are NP-Hard. *J. ACM*, 60(6):45:1–45:39, Nov. 2013.

[16] J. Hora and P. Pudlák. Classification of 9-dimensional trilinear alternating forms over $gf(2)$. *Finite Fields and Their Applications*, 70:101788, 2021.

[17] M. Kauers and J. Moosbauer. Flip Graphs for Matrix Multiplication. In *Proceedings of the 2023 International Symposium on Symbolic and Algebraic Computation*, ISAC '23, pages 381–388, New York, NY, USA, July 2023. Association for Computing Machinery.

[18] M. Kauers and I. Wood. Exploring the Meta Flip Graph for Matrix Multiplication, Oct. 2025.

[19] K. Khoruzhii, P. Gelfß, and S. Pokutta. Faster Algorithms for Structured Matrix Multiplication via Flip Graph Search, Nov. 2025.

[20] T. G. Kolda and B. W. Bader. Tensor decompositions and applications. *SIAM Review*, 51(3):455–500, 2009.

[21] G. Meuli, M. Soeken, E. Campbell, M. Roetteler, and G. D. Micheli. The Role of Multiplicative Complexity in Compiling Low T-count Oracle Circuits, Aug. 2019.

[22] G. Meuli, M. Soeken, and G. De Micheli. Xor-And-Inverter Graphs for Quantum Compilation. *npj Quantum Information*, 8(1):7, Jan. 2022.

[23] J. Moosbauer and M. Poole. Flip Graphs with Symmetry and New Matrix Multiplication Schemes, Feb. 2025.

[24] F. J. R. Ruiz, T. Laakkonen, J. Bausch, M. Balog, M. Barekatain, F. J. H. Heras, A. Novikov, N. Fitzpatrick, B. Romera-Paredes, J. Van De Wetering, A. Fawzi, K. Meichanetzidis, and P. Kohli. Quantum circuit optimization with AlphaTensor. *Nature Machine Intelligence*, 7(3):374–385, Mar. 2025.

[25] P. Selinger. Quantum circuits of T-depth one. *Physical Review A*, 87(4):042302, Apr. 2013.

[26] Y. Shi. Both Toffoli and controlled-NOT need little help to do universal quantum computing. *Quantum Info. Comput.*, 3(1):84–92, Jan. 2003.

[27] V. Vandeaele. Lower T-count with faster algorithms. *Quantum*, 9:1860, Sept. 2025.

[28] V. Vandeaele. Quantum binary field multiplication with subquadratic Toffoli gate count and low space-time cost, Jan. 2025.

[29] E. Witt. Theorie der quadratischen formen in beliebigen körpern. *Journal für die reine und angewandte Mathematik*, 176:31–44, 1937.

11. APPENDIX

A. Flip Graph Connectivity

The flip graph framework of [17] was developed for CP decomposition of a fixed tensor, such as the matrix multiplication tensor. In our setting, the target is not a single tensor but an equivalence class: all tensors T with a prescribed alternating part $\text{Alt}(T) = S$. Equivalently, the cubic phase polynomial defines a trivector $\omega \in \Lambda^3(\mathbb{F}_2^n)$ (an alternating 3-form), and our CP terms (u, v, w) represent decomposable trivectors $u \wedge v \wedge w$ whose sum equals ω . We clarify this distinction and establish that the flip graph remains connected in our setting.

The alternating part of a tensor $T \in \mathbb{F}_2^{n \times n \times n}$ is defined by summing over all permutations of indices:

$$\text{Alt}(T)_{ijk} = T_{ijk} + T_{ikj} + T_{jki} + T_{jik} + T_{kij} + T_{kji}.$$

For distinct i, j, k , this extracts the coefficient of the cubic monomial $x_i x_j x_k$ in f_3 . The diagonal and partially-diagonal entries vanish: $\text{Alt}(T)_{iii} = 0$ and $\text{Alt}(T)_{iij} = 0$ over \mathbb{F}_2 . This motivates calling $S = \text{Alt}(T)$ skew-symmetric rather than symmetric, following the convention that skew-symmetric tensors have zero diagonal.

A CP decomposition $T_{ijk} = \sum_q U_{qi} V_{qj} W_{qk}$ induces a decomposition of the alternating part:

$$S_{ijk} = \sum_q (U_q \wedge V_q \wedge W_q)_{ijk},$$

where the wedge product over \mathbb{F}_2 is defined by

$$(u \wedge v)_{ij} = u_i v_j + u_j v_i.$$

The triple wedge $(u \wedge v \wedge w)_{ijk}$ sums over all six permutations, yielding a fully skew-symmetric rank-1 contribution. Linearly dependent triples satisfy $u \wedge v \wedge w = 0$.

The $\text{GL}(3, 2)$ symmetry means that each rank-1 term (u, v, w) is determined only by the 3-dimensional subspace $\langle u, v, w \rangle$, equivalently by its seven-set (9). Different choices of representative triple from the same seven-set yield different tensors T but the same alternating part S .

We now establish that the flip graph for CP decompositions of cubic phase polynomials is connected. A *split* is the inverse of a reduction: given a term (u, v, w) and any nonzero $w' \in \mathbb{F}_2^n$, we replace (u, v, w) by two terms (u, v, w') and $(u, v, w + w')$. Both configurations contribute the same cubic polynomial, so splits preserve $S = \text{Alt}(T)$. Splits may create duplicate terms; over \mathbb{F}_2 , duplicates cancel and can be removed. A split can be realized by a plus transition followed by a flip, so connectivity via splits implies connectivity via the standard flip graph operations.

Any CP decomposition can be connected to the *standard decomposition* $\{(e_i, e_j, e_k) : S_{ijk} = 1\}$ via splits as follows. Starting from an arbitrary decomposition $\{(u_q, v_q, w_q)\}$, we first split each term by its third factor: for each k with $(w_q)_k = 1$, we split off (u_q, v_q, e_k) . After processing all terms, every third factor is a standard basis vector. We then repeat for the second factor, splitting each (u, v, e_k) into terms (u, e_j, e_k) . Finally, we split by the first factor, obtaining terms (e_i, e_j, e_k) . Since each term is defined only by its subspace, we may reorder indices within each triple to satisfy $i < j < k$. Duplicate

triples cancel over \mathbb{F}_2 , and the remaining terms form the standard decomposition $\{(e_i, e_j, e_k) : S_{ijk} = 1, i < j < k\}$, which depends only on S .

Since every decomposition connects to the standard one via splits, and each split is realized by a plus transition followed by a flip, the flip graph is connected. This parallels Theorem 3.7 of [17], adapted from matrix multiplication tensors to phase polynomial tensors.

B. Symplectic Gaussian Elimination Example

Consider the quadratic form $x_1 x_2 + x_1 x_3 + x_2 x_3$, realized by two *CCZ* gates as shown in Fig. 2b. The corresponding alternating matrix is

$$B = \begin{pmatrix} 0 & 1 & 1 \\ 1 & 0 & 1 \\ 1 & 1 & 0 \end{pmatrix}.$$

Symplectic Gaussian elimination applies simultaneous row and column additions to reduce B to canonical form:

$$\begin{pmatrix} 0 & 1 & 1 \\ 1 & 0 & 1 \\ 1 & 1 & 0 \end{pmatrix} \xrightarrow{3 \leftarrow 3+2} \begin{pmatrix} 0 & 1 & 0 \\ 1 & 0 & 1 \\ 0 & 1 & 0 \end{pmatrix} \xrightarrow{3 \leftarrow 3+1} \begin{pmatrix} 0 & 1 & 0 \\ 1 & 0 & 0 \\ 0 & 0 & 0 \end{pmatrix}.$$

The canonical form contains one 2×2 block, corresponding to the reduced quadratic form $(x_1 + x_3)(x_2 + x_3)$ realized by a single *CCZ* gate.

C. QFT₄ Optimization Details

The QFT₄ circuit is unique among our benchmarks in that its phase polynomial contains linear and quadratic terms alongside cubic terms. Standard Toffoli minimization addresses only the cubic part, leaving residual *T* and *CS* gates. We apply BCO followed by a simple post-processing step: for each *T* gate on variable x_i , we check whether replacing the linear term x_i with $x_i \oplus x_j$ for some j enables cancellation of a *CS* gate. Without this step, BCO produces one additional *CS* gate compared to the reported result. For QFT₄, this combined approach yields an improvement over AlphaTensor-Quantum [24]. This technique is specific to circuits with mixed-degree phase polynomials and was not systematically explored beyond QFT₄.

D. Benchmark Compilation Details

For benchmark circuits in Table 1 where AlphaTensor-Quantum [24] optimized the phase polynomial without circuit splitting, as well as for all 35 circuits from their extended benchmark suite, we used their tensors directly; our CP decompositions are therefore drop-in replacements within their compilation pipeline. For circuits where AlphaTensor-Quantum applied splitting (marked with residual *T* or *CS* gates), we used the Clifford + Phase + Clifford compilation from [27]. For Toffoli minimization, the two compilation approaches yield the same minimum CP rank on all circuits where both apply. For *T*-count minimization, some circuits achieve their minimum only under one of the two compilations; we report the best across both. For planted benchmarks (Fig. 3, 5), tensors were generated directly from sampled decompositions, requiring no circuit compilation.